

# Polyglycerol-poly( $\epsilon$ -caprolactone) block copolymer as a new semi-solid polymeric emulsifier to stabilize O/W nanoemulsions

Hwiseok Jun<sup>1</sup> · Trang Huyen Le Kim<sup>2</sup> · Sang Woo Han<sup>3</sup> · Mintae Seo<sup>2</sup> · Jin Woong Kim<sup>3,4</sup> · Yoon Sung Nam<sup>1,2</sup>

Received: 28 April 2015 / Accepted: 4 June 2015 / Published online: 17 July 2015  
© Springer-Verlag Berlin Heidelberg 2015

**Abstract** This work introduces a new polymeric emulsifier, polyglycerol-*block*-poly( $\epsilon$ -caprolactone), to prepare and stabilize oil-in-water nanoemulsions through the formation of a semi-solid interphase between oil and water. Nanoemulsions are prepared using representative silicone and ester oils, which are widely used for commercial consumer products. The block copolymer is homogeneously solubilized in a mixture of oil and ethanol at 70 °C, and the organic solution is dispersed in water using a conventional homogenizer. Stable nanoemulsions of 220–280 nm in mean diameter are spontaneously generated. The block copolymer is reorganized at the interface to form a robust semi-solid polymeric barrier that can

prevent the entrapped oil from diffusing out to the aqueous phase. The barrier exhibits excellent stability against mechanical stresses, allowing nanoemulsions to be very stable during repeated freeze/thaw cycles. This work suggests that polyglycerol-based block copolymers can be a new promising polymeric emulsifier for stabilization of nanoemulsions of various oils.

**Keywords** Polyglycerol · Amphiphilic copolymers · Nanoemulsions · Polymeric emulsifiers · Dispersion stability

The authors Hwiseok Jun and Trang Huyen Le Kim equally contributed to this work

**Electronic supplementary material** The online version of this article (doi:10.1007/s00396-015-3659-8) contains supplementary material, which is available to authorized users.

✉ Jin Woong Kim  
kjwoong@hanyang.ac.kr

✉ Yoon Sung Nam  
yoonsung@kaist.ac.kr

<sup>1</sup> KAIST Institute for NanoCentury (CNiT), Korea Advanced Institute of Science and Technology, 291 Daehak-ro, Yuseong-gu Daejeon 305-701, Republic of Korea

<sup>2</sup> Department of Materials Science and Engineering, Korea Advanced Institute of Science and Technology, 291 Daehak-ro, Yuseong-gu Daejeon 305-701, Republic of Korea

<sup>3</sup> Department of Bionano Technology, Hanyang University, 55 Hanyangdaehak-ro, Sangnok-gu, Ansan, Gyeonggi-do 426-791, Republic of Korea

<sup>4</sup> Department of Applied Chemistry, Hanyang University, 55 Hanyangdaehak-ro, Sangnok-gu, Ansan, Gyeonggi-do 426-791, Republic of Korea

## Introduction

Stabilization of oil-in-water (O/W) and water-in-oil (W/O) emulsions is affected by electrostatic interactions, steric hindrance, the Marangoni effect, and mechanical forces [1–3]. Surface active molecules, such as surfactants and lipids, are widely used as an emulsifier because their distribution at the interfaces between the two phases is predictable from their molecular structures and controllable by molecular manipulation and combination of multiple compounds. However, the interfaces stabilized by such small molecular weight molecules are intrinsically labile against external stresses. Therefore, polymeric emulsifiers have received much attention as an alternative to surfactants because of low critical micelle concentration (cmc), excellent structural stabilities, and unique conformational properties [4–8]. In addition, they have been considered for biological applications because of biocompatibility, facile surface modification, and stimuli-responsive properties [9–12]. Therefore, various amphiphilic polymers have been studied and used as an emulsifier for industrial applications in the fields of food, cosmetics, drug delivery, etc. [13–16].

In O/W emulsions, a hydrophilic segment of polymeric emulsifiers plays as a corona exposed to the aqueous phase, while a hydrophobic segment anchors to and possibly penetrates into a dispersed oil droplet. Accordingly, the molecular conformation and the penetration depth of a polymer chain into the dispersed phase are critically important for the dispersion stability of emulsions [6, 17, 18]. In general, it is desirable to choose a hydrophobic segment that can be readily dissolved in the dispersed phase to minimize its interactions with solvent molecules in the continuous phase [19]. The conformation of a corona polymer chain also needs to be extended toward the aqueous phase to decrease its undesirable interactions with the dispersed phase [4, 8, 20].

Contrary to this commonly accepted concept, our recent works demonstrated that methoxy poly(ethylene glycol)-*b*-poly( $\epsilon$ -caprolactone) (mPEG-*b*-PCL), where PCL is insoluble in both of the oil and aqueous phases, can be used as an effective emulsifier for various O/W emulsions [21–23]. The block copolymer can be solubilized in ethanol and miscible with oils only at an elevated temperature (about 70 °C). When the oil/polymer mixture was dispersed in an aqueous solution, mPEG-*b*-PCL formed a semi-solid interphase that effectively stabilized O/W emulsions. It was also found that the type of oils greatly affects the morphology and dispersion stability of nanoemulsions [23]. High-pressure homogenization was essential to reduce the size of emulsions to nanoscale for all types of oils tested. Even in the case of micron-sized emulsions, it was very important to apply high-energy inputs in order to stabilize emulsions; otherwise, the block copolymer chains are kinetically frozen within the oil phase and precipitated as semi-crystalline polymer debris rather than migrate to the O/W interface. Although mPEG-*b*-PCL exhibited promising properties as a new type of emulsifier forming a robust semi-solid interphase, high-energy inputs are essential for stabilization of both of nano- and micron-sized emulsions.

In this work, we introduce a new amphiphilic block copolymer, polyglycerol-*b*-poly( $\epsilon$ -caprolactone) (PG-*b*-PCL), as a semi-solid polymeric emulsifier to prepare and stabilize nanoemulsions without high-pressure homogenization. We investigated the impact of a new hydrophilic block on the formation and dispersion stability of O/W nanoemulsions. PG-*b*-PCL was synthesized via the ring opening polymerization of  $\epsilon$ -CL with poly(ethoxyethyl glycidyl ether) (PEEGE) as an initiator, followed by deprotection of PEEGE [24, 25]. Linear and hyperbranched PGs have been widely studied as a hydrophilic corona for anti-fouling coatings and self-assembly of micelle-like structures [24–29]. However, PG has never been used as a corona segment of polymeric emulsifiers for any types of emulsions. This article reports the synthesis and characterization of linear PG-*b*-PCL, and characteristics of its self-assembled micelle-like aggregates in an aqueous solution. We prepared stable nanoemulsions

using PG-*b*-PCL via the formation of a semi-solid interphase at the O/W interface. Dioctanoyl-decanoyl-glycerol (ODO), cethyl ethylhexanoate (CEH), and cyclomethicone (DC345) were used because they are commonly used for cosmetic and personal care products. The prepared nanoemulsions were exposed to a very harsh freeze/thaw cycling condition to examine their dispersion stability against mechanical stresses [30].

## Experimental

### Materials

Glycidol (96 %), *p*-toluenesulfonic acid (TsOH) monohydrate (98.5 %), glycerol (99.5 %), ethyl vinyl ether (98 %), tin(II) 2-ethylhexanoate (Sn(Oct.)<sub>2</sub>, 95 %),  $\epsilon$ -caprolactone (97 %), dichloromethane (anhydrous, 99.8 %), potassium *tert*-butoxide (98 %), and uranyl acetate were purchased from Sigma-Aldrich (St. Louis, MO, USA). For polymerization, glycerol was purified by distillation directly from CaH<sub>2</sub> prior to use. The other reagents and solvents were used as received.

### Methods

#### *Synthesis of PG-*b*-PCL*

Briefly, glycidol and ethyl vinyl ether were used as starting materials and were stirred for 3 min at –30 °C with catalytic amount of TsOH monohydrate. The reaction mixture was magnetically stirred at 25 °C for 3 h. The mixture solution was neutralized by saturated NaHCO<sub>3</sub> solution (68 mL), and the product was extracted twice with ethyl acetate (84 mL  $\times$  2). The organic layer was dried over MgSO<sub>4</sub> and distilled in vacuum at 65 °C to yield ethoxyethyl glycerol ether (EEGE, 1) as a colorless liquid product. The compound 1 was polymerized with potassium *tert*-butoxide as an initiator in THF at –50 °C to give poly(ethoxyethyl glycidyl ether) (PEEGE, 2). After 24 h polymerization, cold methanol (10 °C) was added to the reactor followed by magnetic stirring for 2 h. The resulting polymer which was obtained after the evaporation of methanol and THF was dissolved in hexane and centrifuged at 3500 rpm for 10 min to remove the precipitated potassium chloride. Compound 2 was obtained by drying in vacuum for 24 h. The following polymerization reaction of compound 2 with  $\epsilon$ -caprolactone monomer gave PEEGE-*b*-PCL (3) block copolymer. The reaction was catalyzed by tin(II) 2-ethylhexanoate (1.15 g, 3 wt.% of PEEGE +  $\epsilon$ -caprolactone). After a step for removal of impurities by centrifuge, the desired block copolymer (3) was obtained by precipitation in cold hexane. Finally, PEEGE groups in compound 3 were deprotected to produce polyglycerol groups, and the whole block copolymer could be PG-*b*-PCL (4).

Addition of oxalic acid in acetone broke down ether bonds in PEEGE groups, and the final block copolymer was obtained by dialysis against an excess amount of water (MWCO = 1 kDa) at room temperature for 1 day.

#### Characterization of PG-*b*-PCL

The successful synthesis of the polymer was confirmed with Fourier transform-infrared spectroscopy (ALPHA FT-IR Spectrometer with a diamond ATR probe, Bruker, Billerica, MA, USA). The molecular weight of the synthesized polymer was determined using gel permeation chromatography (GPC). A high-performance liquid chromatography (HPLC) system composed of Agilent 110 series (Agilent Technologies, Palo Alto, CA, USA) and refractive index detector was operated at  $1.0 \text{ mL min}^{-1}$  using a series of three PLgel columns ( $300 \times 7.5 \text{ mm}$ , pore sizes =  $10^3$ ,  $10^4$ , and  $10^5 \text{ \AA}$ ). Tetrahydrofuran was used as an isocratic mobile phase, and monodisperse polystyrenes (Polysciences, Inc., Warrington, PA, USA) were used as calibration standards.  $^1\text{H}$  nuclear magnetic resonance (NMR) spectrum was obtained at  $25 \text{ }^\circ\text{C}$  with a Bruker NMR operating at 300 MHz using  $\text{CDCl}_3$  as a solvent. Chemical shifts were measured in parts per million (ppm). Thermal properties of the synthesized polymers were analyzed by differential scanning calorimeter (DSC) using DSC 204 F1 Phoenix (Netzsch-Gerätebau GmbH, Selb, Germany). Two scan circles of heating and cooling were run between  $-50 \text{ }^\circ\text{C}$  to  $200 \text{ }^\circ\text{C}$  at a scan rate of  $10 \text{ }^\circ\text{C min}^{-1}$ . Data from second heating were analyzed to determine the enthalpy of endothermic processes.

#### Preparation and characterization of PG-*b*-PCL micelle-like aggregates

To prepare micelle-like aggregates, polymer powders (10 mg) were dissolved in acetone at a concentration of  $10 \text{ mg mL}^{-1}$ , and then the polymer solution was added to 10 mL of deionized water with vigorous stirring. The prepared solution was left at room temperature overnight to completely evaporate the organic solvent. A series of self-assembled micelle-like aggregates of PG-*b*-PCL with different concentrations was prepared via serial dilution with deionized water to determine the cmc as previously reported [31]. Two milligrams of pyrene was dissolved in 20 mL ethanol and diluted with deionized water to the final concentration of 0.5 mM. Two milliliters of this solution was diluted with 8 mL of deionized water, and 1 mL of the resulting solution was diluted again with 49 mL of deionized water. Subsequently, 100  $\mu\text{L}$  of a pyrene solution (2  $\mu\text{M}$ ) was added to 900  $\mu\text{L}$  of PG-*b*-PCL solutions. Fluorescence intensities were measured by a fluorescence spectrophotometer F7000 (Hitachi, Tokyo, Japan) using a quartz cell. Fluorescence spectra were recorded from 350 to 450 nm with excitation at 332 nm. Scan speed was set at  $240 \text{ nm min}^{-1}$ , and

the slit width was 5 nm for both excitation and emission. The peak intensities at 372 and 384 nm were collected, and their ratios ( $I_{372}/I_{384}$ ) were recorded as a function of the block copolymer concentration. The cmc values were calculated using a sigmoidal (Boltzmann type) fitting curve.

#### Preparation of O/W nanoemulsions

Ten milligrams of PG-*b*-PCL and 100 mg of oil were dissolved completely in 1 mL of ethanol in a sonication bath at  $70 \text{ }^\circ\text{C}$  for 15 min. The solution was dropped slowly into 5 mL of deionized water with high-speed homogenization using a Wise Tis HG-15A homogenizer (witeg Labortechnik GmbH, Wertheim, Germany) at 10,000 rpm for 5 min at  $70 \text{ }^\circ\text{C}$ . Then the mixture was stirred in air until cooled to an ambient temperature.

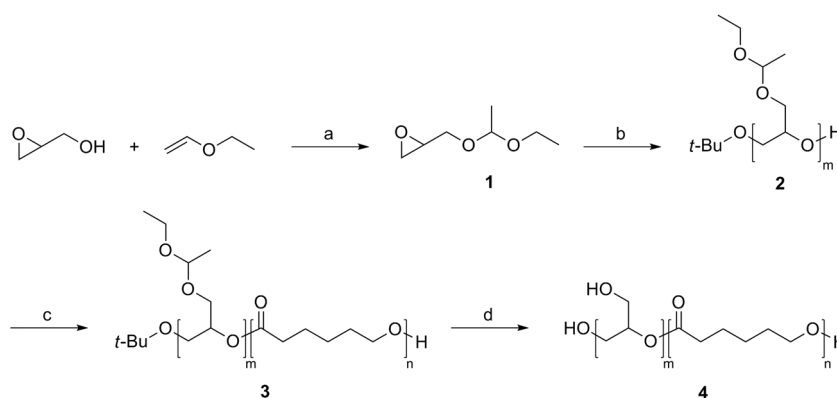
#### Dynamic light scattering and transmission electron microscopy

Size distributions were measured at  $25 \text{ }^\circ\text{C}$  by dynamic laser light scattering (DLS) using a zeta potential and particle size analyzer ELSZ-1000 (Otsuka Electronics Co., Ltd., Osaka, Japan). Hydrodynamic diameter was determined using the CONTIN algorithm. The second-order polydispersity index ( $\mu_2/I^2$ ), where  $\mu$  is the second moment about the mean and  $I$  is the average decay rate, determined using the method of cumulants. Transmission electron microscope (TEM) was also used to observe the particle morphologies. Five microliters of nanoemulsion samples were mixed with 10  $\mu\text{L}$  of 1 % uranyl acetate for negative staining, then that mixture was placed onto a copper grid coated with carbon followed by incubation for 20 min at room temperature. The drop was then removed by touching to a filter paper and the grid was air dried for 20 min. The samples were observed by Electron Microscope JEM 3010 (JEOL, Akishima, Japan) operated at 300 kV.

## Results and discussion

PG-*b*-PCL was synthesized via the combination of anionic polymerization and ring opening polymerization as shown in Fig. 1. Firstly, glycidol was conjugated to ethyl vinyl ether in order to obtain EEGE (yield = 75.6 %) in the presence of PTSA at room temperature. Then, PEEGE was synthesized by anionic polymerization of EEGE using potassium *tert*-butoxide as an initiator, as established by Dworak et al. [32]. The weight average molecular weight ( $M_w$ ) and polydispersity index (PDI) of the produced PEEGE were 3.7 kDa and 1.46, respectively. The yield of this reaction was around 90 % in weight. The terminal hydroxyl group of PEEGE was used as an initiator for ring opening polymerization of  $\epsilon$ -

**Fig. 1** **a** *p*-Toluenesulfonic acid, 25 °C, 3 h; **b** potassium *tert*-butoxide, THF, 65 °C, 24 h; **c**  $\epsilon$ -caprolactone, tin(II) 2-ethylhexanoate, neat, 125 °C, 20 h; and **d** oxalic acid, acetone, room temperature, 5 h



caprolactone in the presence of tin(II) 2-ethylhexanoate as a catalyst. The synthesized PEEGE-*b*-PCL was purified by precipitation in an excess amount of cold *n*-hexane. The  $M_w$  and PDI were 13.5 kDa and 2.48, respectively, as determined by GPC. The protecting acetal groups in the PEEGE block were cleaved by acidic hydrolysis with oxalic acid in acetone. Then, the reaction mixture was dialyzed against an excess amount of deionized water to obtain pure PG-*b*-PCL. The synthesized PG-*b*-PCL was soluble in chloroform while insoluble in DMSO and methanol (Supplementary data, Table S1).

$^1\text{H}$  NMR spectrum of the synthesized PG-*b*-PCL shows the peak number 1 to 5 for the hydrogen atoms in the PCL segment and broad peaks of 6 to 8 for those in the PG segment (Fig. 2a and Fig. S1). This spectrum confirms the existence of both of the PG and PCL segments in the final product. The molar ratio of PCL to PG was 2.44, corresponding to a weight ratio of 3.85. The  $M_w$  and PDI were 17 kDa and 1.51, respectively. In addition, the presence of a hydroxyl group on PG-*b*-PCL was confirmed through FT-IR (wavenumber = 3300–3400  $\text{cm}^{-1}$ , Fig. 2b). The thermal properties of both of PCL and PG-*b*-PCL were examined using DSC (Fig. 2c). Splitting of the endothermic melting peak was observed for both of the polymers. This phenomenon indicates the existence of two different crystalline phases in the PCL block, which can be caused by heterogeneous nucleation due to spatial confinement [33]. The melting temperature of PCL in the block copolymer significantly decreased (1st, 58.3 °C and 2nd, 51.6 °C) compared to that of free PCL powders (1st, 68.4 °C and 2nd, 54.2 °C). The enthalpy in PG-*b*-PCL (1st,  $-93.04$  J/g and 2nd,  $-70.59$  J/g) was also significantly lower than that in PCL (1st,  $-102.2$  J/g and 2nd,  $-75.15$  J/g). These results indicate that the presence of the PG block effectively interfered with the crystallization of PCL.

The cmc of PG-*b*-PCL in deionized water was determined from the characteristic band shift in the fluorescence spectra of pyrene upon its partition into the inner core of micelles (Fig. S2). Figure 3a shows the intensity ratios ( $I_{372}/I_{384}$ ) of pyrene excitation spectra versus the logarithm of polymer concentration ( $\log_{10} C$ ). The cmc was obtained from the intersection of two straight lines: the base line and the rapidly

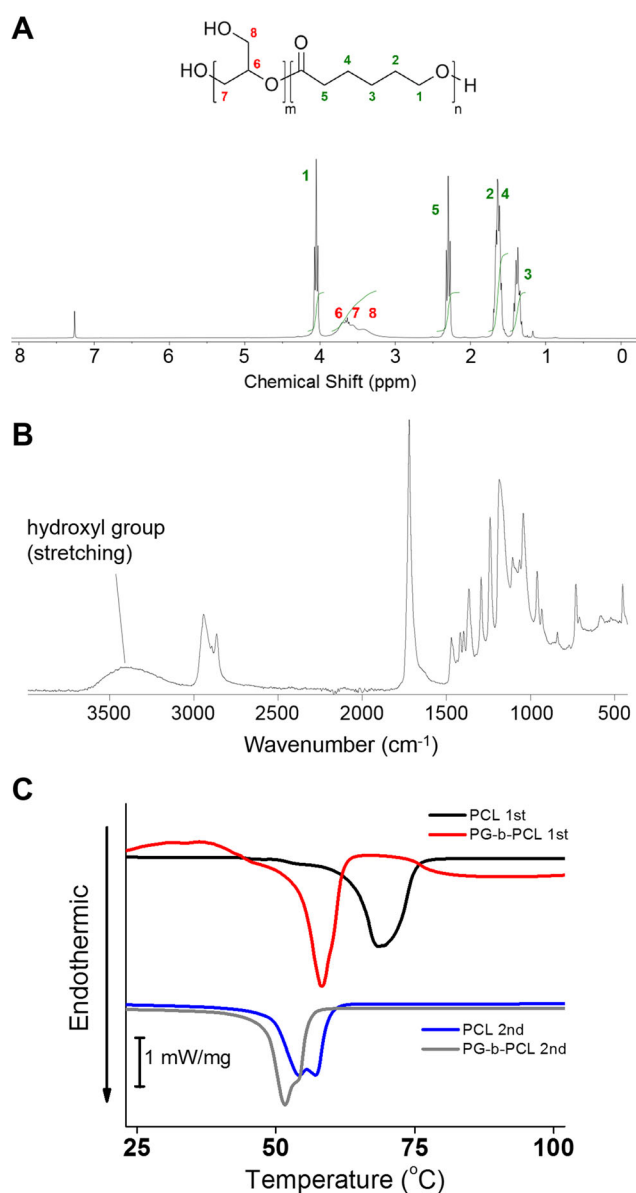
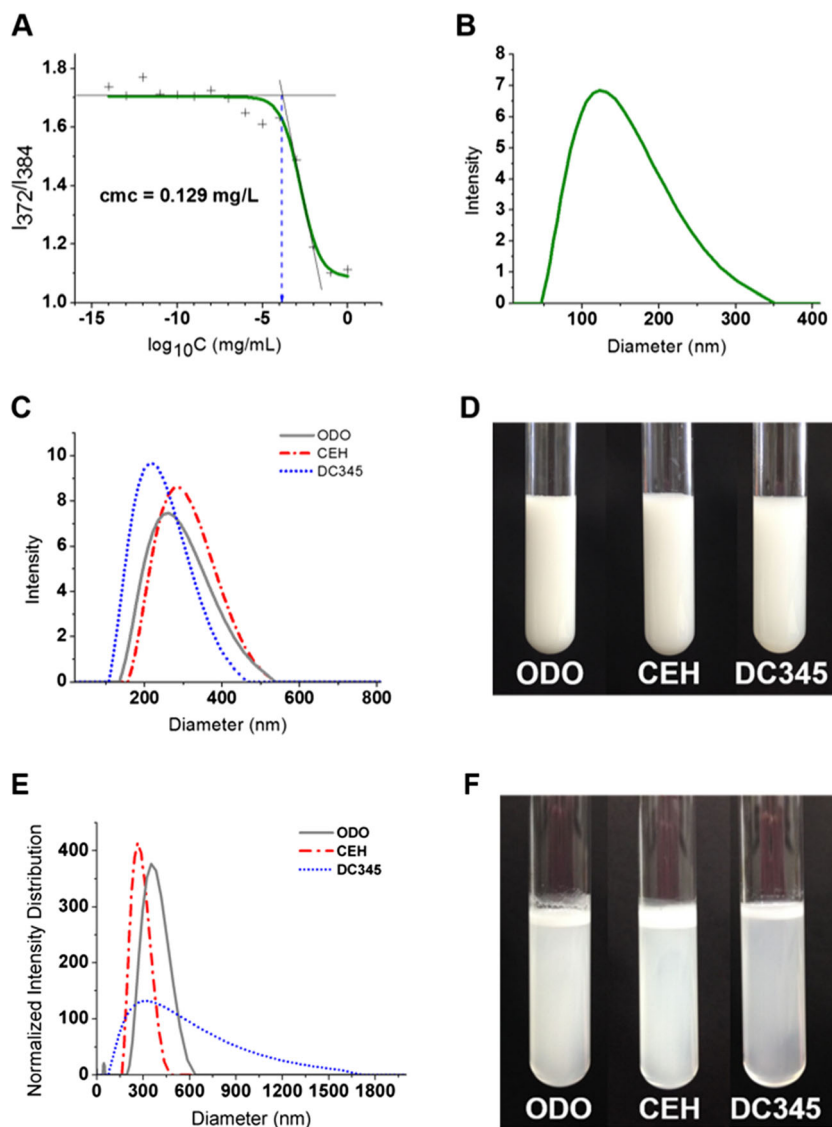


**Fig. 2** **a** Chemical structure of PG-*b*-PCL with its  $^1\text{H}$  NMR spectrum in  $\text{CDCl}_3$ . **b** FT-IR absorbance spectrum of PG-*b*-PCL. **c** DSC diagram of the first and second heating scans of PG-*b*-PCL



**Fig. 3** **a** Critical micelle concentration of PG-*b*-PCL derived from the fluorescence of pyrene. **b** Size distribution of PG-*b*-PCL micelles in an aqueous solution with 1 mg/1 mL concentration. Size distribution (c) and a digital photograph (d) of PG-*b*-PCL nanoemulsions of ODO, CEH, and DC345. Size distribution (e) and a digital photograph (f) of mPEG-*b*-PCL nanoemulsions of the same oils



falling intensity ratio [31]. Because of a relatively large Mw (17 kDa) and a high weight ratio of hydrophobic to hydrophilic blocks (3.85), the measured cmc was very low ( $1.29 \times 10^{-4} \text{ g L}^{-1}$ ) in deionized water. This value is much smaller than those of non-ionic surfactants (e.g.,  $7.4 \times 10^{-2} \text{ g L}^{-1}$  for Tween 20,  $2.0 \times 10^{-1} \text{ g L}^{-1}$  for Triton X-100, and  $1.1 \text{ g L}^{-1}$  for Brij 35) [34] and even relatively smaller than those of other micelle-like polymeric aggregates (e.g.,  $2.6\text{--}8 \text{ g L}^{-1}$  for Pluronic F127) [35]. Accordingly, the size of the micelle-like aggregates of PG-*b*-PCL was larger than that of conventional surfactants. The hydrodynamic mean diameter of PG-*b*-PCL aggregates was about 111 nm with a second-order polydispersity index ( $\mu_2/I^2$ ) of 0.18, indicating a narrow size distribution. The surface of PG-*b*-PCL aggregates was slightly negatively charged as indicated by a zeta potential of about  $-5.78 \text{ mV}$  in water (Fig. S3).

The diameter was increased when oils were added to the ethanolic solution of PG-*b*-PCL compared to the diameter of

micelle, and chemical structures of oils were described in Fig. S4. To prepare nanoemulsions, the synthesized diblock copolymers were dissolved in ethanol at  $70^\circ\text{C}$  and then mixed with the oils mentioned above. No phase separation was observed for all of the oils tested at the temperature. The homogeneous oil/polymer mixtures were poured into deionized water at  $70^\circ\text{C}$  with homogenization at 10,000 rpm for 5 min, generating nano-sized embryonic droplets immediately. The solidification of the polymer chains occurred rapidly as they diffuse out of the organic phase toward the O/W interface, where the hydrophilic block in the polymer chain could stretch into the aqueous phase. The ethanol in the droplet also diffuses into water very fast because of its small molecular size and high miscibility with water, leaving the hydrophobic block in the oil phase. Nanoemulsions were successfully prepared using PG-*b*-PCL as a semi-solid emulsifier for all of the oils tested in this work. The mean hydrodynamic diameters of ODO, CEH, and DC345 nanoemulsions stabilized with PG-

*b*-PCL were 246, 278, and 226 nm, respectively (Fig. 3c). The photograph of the prepared nanoemulsions shows that there was no apparent phase separation (Fig. 3d). As a control experiment, mPEG-*b*-PCL was used as an emulsifier to prepare nanoemulsions of the same oils following the same experimental procedures. The  $M_w$  of mPEG-*b*-PCL was 13,660 Da with a PDI of 1.22. The molar ratio of mPEG to PCL was 2.72, corresponding to a weight ratio of 1.05. This polymer was successfully employed to prepare highly stable nanoemulsions when high-pressure homogenization at a pressure of about 1 kbar as shown in our previous work [23]. However, conventional homogenization at 10,000 rpm resulted in immediate phase separation of the resulting nanoemulsions (Fig. 3e, f), indicating the importance of processing conditions in the preparation of stable nanoemulsions using mPEG-*b*-PCL. Stabilization of the O/W interface with the block copolymer could be kinetically determined by the competition between the insolubilization of the polymer chains within the organic phase and their migration toward the O/W interface. Therefore, the successful stabilization of nanoemulsions by PG-*b*-PCL with relatively mild homogenization suggests that the choice of a hydrophilic segment can be a very important factor that determines the solubility (and wettability) of polymers in oils and self-organization of the amphiphilic block copolymer at the interface.

Apparent macroscopic phase separation (creaming) was observed for the CEH nanoemulsions after incubation at room temperature in 1 day, while the ODO and DC345 nanoemulsions still exhibit homogeneous appearance

(Fig. 4a, b). Note that the hydrodynamic diameter of the CEH nanoemulsions (278 nm) was larger than those of the other nanoemulsions (246 nm for ODO and 226 nm for DC345) when the size was measured immediately after preparation. Relatively fast creaming of the CEH nanoemulsions was observed from repeated experiments several times. One possible factor that induced such destabilization is a relatively larger difference of oil density [36]. The specific gravity of CEH is 0.86 at 25 °C while those of ODO and DC345 are 0.94 and 0.96, respectively. CEH also has a relatively low viscosity (13 mPa s, 25 °C) compared to the other oils (70 mPa s for ODO and 20 mPa s for DC345). The low density and viscosity of CEH are disadvantageous for the prevention of Ostwald ripening, which is a major mechanism of destabilization of nanoemulsions [37]. However, despite these disadvantages, CEH was very successfully emulsified into stable nanoemulsions with mPEG-*b*-PCL, as shown in our previous work, indicating that the large density difference and low viscosity are not likely features that exclusively determine the dispersion stability of nanoemulsions prepared using a semi-solid polymer emulsifier [23].

The wettability of the polymer chains by oils can be another important factor to be considered because the types of oil significantly affected the stability of nanoemulsions [23]. If the phase separation between polymer and oil occurs very quickly, PG-*b*-PCL can be precipitated in the organic phase rather than migrate to the O/W interface. To determine the amount of oil absorbed by PG-*b*-PCL, 100 mg of PG-*b*-PCL was mixed with 1 g of ODO, CEH, and DC345, respectively. The mixtures were kept at 80 °C for 24 h and then vortexed vigorously. The mixtures were then cooled down to room temperature. At 80 °C, the oil/polymer mixtures were homogeneously transparent without any phase separation. However, when they were cooled down to room temperature, the semi-solid oil/polymer mixture was completely separated from the oil phase in the case of CEH and DC345. In contrast, the ODO/PG-*b*-PCL mixture formed a gel-like structure, indicating that the PCL block is highly wettable by ODO, which has a chemical structure similar to the repeated ester unit of PCL. The weight percentages of oil in the semi-solid oil/polymer mixtures were 90.2, 35.3, and 39.8 %, for ODO, CEH, and DC345, respectively (Fig. S5). No significant differences in the wettability of PG-*b*-PCL between CEH and DC345 suggest that the oil wettability is not the sole parameter that determines the destabilization of the CEH nanoemulsions.

Although the underlying mechanism on destabilization of the CEH nanoemulsions is not clearly understood, one phenomenological feature is that destabilized emulsions have very heterogeneous surface structures. TEM images showed that the CEH nanoemulsions have irregular small domains, which seem to be polymer-rich phases separated from the organic phase (Fig. 4b). These irregular small particle-like structures were also observed for other unstable

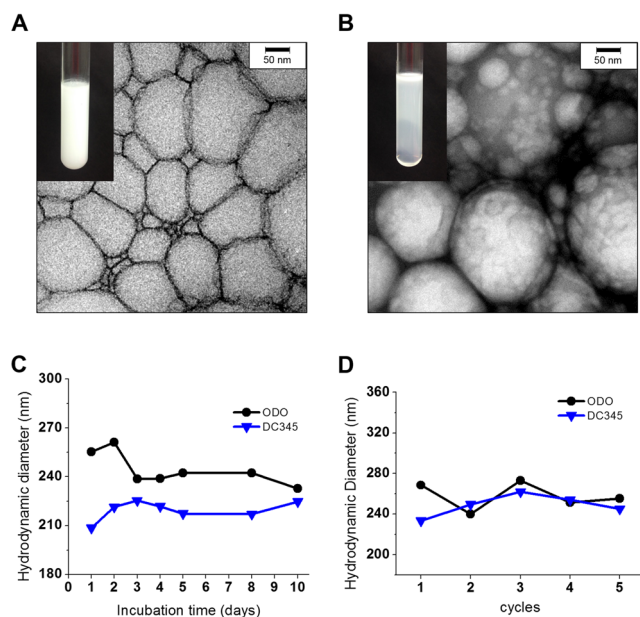


**Fig. 4** TEM images with digital photographs of O/W nanoemulsions of ODO (a) and CEH (b) stabilized with PG-*b*-PCL. Time-dependent evolution of the hydrodynamic diameters of O/W nanoemulsions stabilized with PG-*b*-PCL through 10 days at room temperature (c) and 5 cycles of freeze/thaw processes (d)

nanoemulsions; for example, nanoemulsions of isopropyl myristate and liquid paraffin prepared using mPEG-*b*-PCL by high-pressure homogenization [23]. In these cases, the unstable interface was ascribed to fast precipitation of the polymer chains in the organic phase due to the incompatibility of the PCL block with the oils. However, the instability of the CEH nanoemulsions raised another possibility that the interaction between the hydrophilic block and oil is also an important factor for dispersion stability of nanoemulsions. It should be noted that PG-*b*-PCL contains a hydroxyl group in each monomeric unit, which can provide a proton donor for hydrogen bonding to the oxygen in the ester linkage of CEH. The existence of hydrogen bonding between PG and CEH can interfere with the extension of the hydrophilic chain to the aqueous phase, resulting in much less effective repulsion between neighboring hydrophilic chains. Further study is underway to clarify the effects of oil on the intermolecular association of the hydrophilic chains of the polymeric emulsifier, which needs to be suppressed for effective steric repulsion between oil droplets.

The dispersion stability of the ODO and DC345 nanoemulsions was examined under two different conditions: (1) incubation at room temperature for 10 days (Fig. 4c) and (2) a repeated freeze/thaw cycling process (Fig. 4d). The nanoemulsions were incubated without using any additional agents, such as thickeners and organic solvents. Slight fluctuation in the emulsion size was observed for both of the nanoemulsions during incubation for 10 days, but there was no tendency to either the increased size of nanoemulsions or any apparent phase separation. In particular, both of the nanoemulsions exhibited excellent stability during repeated freeze/thaw cycles, which generate a high level of mechanical stresses to the emulsions. These results suggest that the nanoemulsions stabilized with PG-*b*-PCL have a very robust interphase, effectively preventing oil from diffusing out to the aqueous phase.

## Conclusions

It was demonstrated that a polyglycerol-based block copolymer, PG-*b*-PCL, can effectively stabilize O/W nanoemulsions through the formation of a semi-solid interphase. Nanoemulsions were prepared using three different ester and silicone oils (ODO, CEH, and DC345), all of which are commonly used for cosmetic and personal care products. The block copolymer is homogeneously solubilized in a mixture of ethanol and oil at 70 °C. The organic solution is dispersed in water by homogenization at 10,000 rpm. The block copolymer is reorganized at the interface to form a robust semi-solid polymeric barrier between oil and water. The dispersion stability of the prepared nanoemulsions was dependent upon the oil type. While the nanoemulsions exhibited macroscopic

phase separation for CEH, there was no significant change of appearance and emulsion sizes in the ODO and DC345 nanoemulsions. The surface of these stable nanoemulsions was very smooth, indicating no microscopic phase separation, allowing nanoemulsions to exhibit excellent stability against mechanical stresses generated during repeated freeze/thaw cycles. This work suggests that PG-*b*-PCL is an attractive emulsifier for nanoemulsions that require structural stability under various stresses.

**Acknowledgments** This study was supported by a grant of the Korea Healthcare Technology R&D Project, Ministry of Health & Welfare, Republic of Korea (Grant No.: HN12C0064).

## References

- Ivanov IB, Kralchevsky PA (1997) Stability of emulsions under equilibrium and dynamic conditions. *Colloids Surf., A* 128:155–175
- Wilde PJ (2000) Interfaces: their role in foam and emulsion behaviour. *Curr. Opin. Colloid Interface Sci.* 5:176–181
- Karakashev SI, Manev ED, Tsekov R, Nguyen AV (2008) Effect of ionic surfactants on drainage and equilibrium thickness of emulsion films. *J. Colloid Interface Sci.* 318:358–364
- Tadros TF, Vandamme A, Leveck B, Booten K, Stevens CV (2004) Stabilization of emulsions using polymeric surfactants based on inulin. *Adv. Colloid Interface Sci.* 108–109:207–226
- Bobin M, Michel V, Martini M (1999) Study of formulation and stability of emulsions with polymeric emulsifiers. *Colloids Surf., A* 152:53–58
- Barnes TJ, Prestidge CA (2000) PEO-PPO-PEO block copolymers at the emulsion droplet-water interface. *Langmuir* 16:4116–4121
- Yonekura K, Hayakawa K, Kawaguchi M, Kato T (1998) Preparation of stable silicone oil emulsions in the presence of hydroxypropyl methyl cellulose. *Langmuir* 14:3145–3148
- Hanson JA, Chang CB, Graves SM, Li Z, Mason TG, Deming TJ (2008) Nanoscale double emulsions stabilized by single-component block copolypeptides. *Nature* 455:85–88
- Nam YS, Kang HS, Park JY, Park TG, Han SH, Chang IS (2003) New micelle-like polymer aggregates composed of PEI-PLGA diblock copolymers: micellar characteristics and cellular uptake. *Biomaterials* 24:2053–2059
- Yeom J, Nam YS (2012) Self-assembled, pH-sensitive retinoate nanostructures ionically complexed with PEG-grafted cationic polyelectrolytes. *Colloid Polym. Sci.* 290:839–845
- Mathur AM, Drescher B, Scranton AB, Klier J (1998) Polymeric emulsifiers based on reversible formation of hydrophobic units. *Nature* 392:367–370
- Oh MH, Kim JS, Lee JY, Park TG, Nam YS (2013) Radio-opaque theranostic nanoemulsions with synergistic anti-cancer activity of paclitaxel and Bcl-2 siRNA. *RSC Adv.* 3:14642–14651
- de Medeiros MS, Otsuka I, Fort S, Minatti E, Borsali R, Halila S (2012) Sweet block copolymer nanoparticles: preparation and self-assembly of fully oligosaccharide-based amphiphile. *Biomacromolecules* 13:1129–1135
- Klaikherd A, Nagamani C, Thayumanavan S (2009) Multi-stimuli sensitive amphiphilic block copolymer assemblies. *J. Am. Chem. Soc.* 131:4830–4838
- Gao C, Li S, Li Q, Shi P, Shah SA, Zhang W (2014) Dispersion RAFT polymerization: comparison between the monofunctional

- and bifunctional macromolecular RAFT agents. *Polym. Chem.* 5: 6957–6966
16. Fang JY, Hung CF, Hua SC, Hwang TL (2009) Acoustically active perfluorocarbon nanoemulsions as drug delivery carriers for camptothecin: Drug release and cytotoxicity against cancer cells. *Ultrasonics* 49:39–46
  17. Liu S, Armes SP (2001) Recent advances in the synthesis of polymeric surfactants. *Curr. Opin. Colloid Interface Sci.* 6:249–256
  18. March GC, Napper DH (1977) The thermodynamic limit to the flocculation stability of sterically stabilized emulsions. *J. Colloid Interf. Sci.* 61:383–387
  19. Sela Y, Magdassi S, Garti N (1994) Newly designed polysiloxane-graft-poly(oxyethylene) copolymeric surfactants: preparation, surface activity and emulsification properties. *Colloid Polym. Sci.* 272: 684–691
  20. Capek I (2004) Degradation of kinetically-stable o/w emulsions. *Adv. Colloid Interface Sci.* 107:125–155
  21. Nam YS, Kim JW, Park J, Shim J, Lee JS, Han SH (2012) Tocopheryl acetate nanoemulsions stabilized with lipid-polymer hybrid emulsifiers for effective skin delivery. *Colloids Surf., B* 94:51–57
  22. Nam YS, Kim JW, Shim J, Han SH, Kim HK (2010) Silicone oil emulsions stabilized by semi-solid nanostructures entrapped at the interface. *J. Colloid Interf. Sci.* 351:102–107
  23. Nam YS, Kim JW, Shim J, Han SH, Kim HK (2010) Nanosized emulsions stabilized by semisolid polymer interphase. *Langmuir* 26:13038–13043
  24. Imran ul-haq M, Lai BFL, Chapanian R, Kizhakkedathu JN (2012) Influence of architecture of high molecular weight linear and branched polyglycerols on their biocompatibility and biodistribution. *Biomaterials*, 33:9135–9147.
  25. Weinhart M, Grunwald I, Wyszogrodzka M, Gaetjen L, Hartwig A, Haag R (2010) Linear poly(methyl glycol) and linear polyglycerol as potent protein and cell resistant alternatives to poly(ethylene glycol). *Chem. Asian J.* 5:1992–2000
  26. Wilms D, Stiriba SE, Frey H (2009) Hyperbranched polyglycerols: from the controlled synthesis of biocompatible polyether polyols to multipurpose applications. *Acc. Chem. Res.* 43:129–141
  27. Lee S, Saito K, Lee HR, Lee MJ, Shibasaki Y, Oishi Y, Kim BS (2012) Hyperbranched double hydrophilic block copolymer micelles of poly(ethylene oxide) and polyglycerol for pH-responsive drug delivery. *Biomacromolecules* 13:1190–1196
  28. Wurm F, Klos J, Rader HJ, Frey H (2009) Synthesis and noncovalent protein conjugation of linear-hyperbranched PEG-poly(glycerol)  $\alpha, \omega_n$ -telechelics. *J. Am. Chem. Soc.* 131:7954–7955
  29. Wyszogrodzka M, Haag R (2009) Study of single protein adsorption onto monoamino oligoglycerol derivatives; a structure-activity relationship. *Langmuir* 25:5703–5712
  30. Donsi F, Wang Y, Huang Q (2011) Freeze-thaw stability of lecithin and modified starch-based nanoemulsions. *Food Hydrocolloids* 25: 1327–1336
  31. Basu Ray G, Chakraborty I, Moulik SP (2006) Pyrene absorption can be a convenient method for probing critical micellar concentration (cmc) and indexing micellar polarity. *J. Colloid Interf. Sci.* 294: 248–254
  32. Dworak A, Panchev I, Trzebicka B, Walach W (1998) Poly(alpha-tau-butoxy-omega-styrylo-glycidol): a new reactive surfactant. *Polym. Bull.* 40:461–468.
  33. Suzuki Y, Duran H, Akram W, Steinhart M, Floudas G, Butt HJ (2013) Multiple nucleation events and local dynamics of poly( $\epsilon$ -caprolactone) (PCL) confined to nanoporous alumina. *Soft Matt.* 9: 9189–9198
  34. Hait S, Moulik S (2001) Determination of critical micelle concentration (CMC) of nonionic surfactants by donor-acceptor interaction with iodine and correlation of CMC with hydrophile-lipophile balance and other parameters of the surfactants. *J. Surfactants Deterg.* 4:303–309
  35. Gao Q, Liang Q, Yu F, Xu J, Zhao Q, Sun. B (2011) Synthesis and characterization of novel amphiphilic copolymer stearic acid-coupled F127 nanoparticles for nano-technology based drug delivery system. *Colloids Surf., B*, 88:741–748.
  36. Murakami R, Moriyama H, Noguchi T, Yamamoto M, Binks BP (2014) Effects of the density difference between water and oil on stabilization of powdered oil-in-water emulsions. *Langmuir* 30: 496–500
  37. Wooster TJ, Golding M, Sanguansri P (2008) Impact of oil type on nanoemulsion formation and Ostwald ripening stability. *Langmuir* 24:12758–12765